for FIFC in 18 May, 2007
Ver. 2007-05-07

Report on Technical Issues for J-PARC E10 Experiment

Contents

1 J-PARC E10 Experiment and Requirements

The J-PARC E10 experiment "Production of Neutron-Rich Λ-Hypernuclei with the Double Charge-Exchange Reaction" aims to produce new neutron-rich Λ-hypernuclei and study hypernuclear structures by using the double charge-exchange reaction, the (π^-, K^+) reaction [1]. This is the first attempt to produce Λ-hypernuclei quite close to the neutron-drip line, and the hypernuclear structures of such neutron-rich Λ-hypernuclei are important inputs to discuss the Λ-N interaction in the neutron-rich environment or in the high isospin state.

The double charge-exchange reaction was successfully used to produce a neutron-rich hypernucleus ${}^{10}_{\Lambda}$Li at KEK-PS (KEK-PS-E521 experiment) [2]. In the J-PARC E10 experiment, we would like to extend the study to other neutron-rich hypernuclei, ${}^{9}_{\Lambda}$He and ${}^{6}_{\Lambda}$H. The feasibility of the E10 experiment is discussed in this report based on the information obtained in the E521 experiment together with performances of facilities and detectors to be available at J-PARC.

1.1 Requirement on experimental yield

One of important information obtained in the previous E521 experiment was the production cross section of the neutron-rich Λ-hypernucleus by the double charge-exchange (π^-, K^+) reaction. Table 1 shows a summary of typical production cross sections of hypernuclei by several reactions. As one can see, the production cross

Table 1: Summary of cross sections for several reactions for the production of hypernuclei. Beam momenta are 1.05, 1.2 and 0.9 GeV/c for the (π^+, K^+), (π^-, K^+) and (K^-, π^-) reactions, respectively.

	typical cross section			
process	(π^+, K^+)	(π^-, K^+)	(K^-, π^-)	(K^-, π^+)
production of hypernuclei	8 μb/sr	10 nb/sr	200 μb	n.a.
elementary process	0.4 mb/sr	–	4 mb/sr	–

section of the (π^-, K^+) reaction is very small, about 10 nb/sr or 1/1000 of the (π^+, K^+) reaction cross section. This tiny cross section of the double charge-exchange reaction is one of difficulties in the measurement. Actually, the yield of the ${}^{10}_{\Lambda}$Li hypernucleus production was only 47 events in the E521 experiment.

In the E10 proposal, we estimated the yield of the ${}^{9}_{\Lambda}$He hypernucleus as follows:

$$Yield\ ({}^{9}_{\Lambda}\mathrm{He}) = N_{Beam} \times \frac{N_{Target}}{9} \times N_A \times \frac{d\sigma}{d\Omega} \times \Omega_{SP} \times \varepsilon_{SP} \times \varepsilon_{Anal} \times \frac{Time}{T_{Cycle}} \quad (1)$$

If we employ parameters listed in Table 2 we expect about 310 events in 3 weeks of beamtime. This yield is roughly one order of magnitude larger compared with that

Table 2: Basic parameters for the ${}^{9}_{\Lambda}$He hypernucleus production.

Parameters	Values	Notation in Eq.(1)
π^- beam momentum	1.20 GeV/c	
π^- beam intensity	1×10^7 /spill	N_{Beam}
PS acceleration cycle	3.4 sec	T_{Cycle}
^{9}Be target thickness	3.5 g/cm^2	N_{Target}
Reaction cross section	10 nb/sr	$d\sigma/d\Omega$
Spectrometer solid angle	0.1 sr	Ω_{SP}
Spectrometer efficiency	0.5	ε_{SP}
Analysis efficiency	0.5	ε_{Anal}

in the previous experiment, and the improvement in the yield is inevitable to discuss the structure of the neutron-rich hypernuclei much more clearly. So, we consider the yield of about 300 events as one of baselines of the design of the experiment. The discussion on the design of the experiment to obtain the yield is made in more detail in Sec.2.2.

1.2 Energy resolution for identification of hypernuclei

The hypernuclear spectroscopy is usually made by using the missing mass method. In the case of the (π^-, K^+) reaction, the momenta of a π^- beam and an ejectile K^+ have to be measured to estimate the missing mass M_X by assuming the A(π^-, K^+)X kinematics. The missing mass distribution reflects the binding energy and structure of hypernuclei. The precision of the momentum measurements of π^- and K^+ determines the missing mass resolution.

The production of hypernuclei always accompanies the Λ quasi-free production process, N$\pi \rightarrow \Lambda K$ process, and the quasi-free production cross section is usually larger than that of the production of hypernuclei. We can distinguish the hypernuclear states from the quasi-free Λ production component only by the difference of the missing mass. So, a good missing mass or excitation energy resolution is necessary to see the hypernuclear structure clearly. The energy resolution is much more critical for the structure study of the ${}^{6}_{\Lambda}$H hypernucleus because the ground state binding energy will be smaller than that of the ${}^{9}_{\Lambda}$He and ${}^{10}_{\Lambda}$Li hypernuclei and the core nucleus ^{5}H is unbound. If the binding energy is smaller, the ground state peak comes closer to the tail of the quasi-free process.

Figure 1 shows energy thresholds of various particle decay channels in the neutron-rich hypernuclei, ${}^{9}_{\Lambda}$He (left) and ${}^{6}_{\Lambda}$H (right), measured from the ground states. The ground state binding energies were not known yet for the neutron-rich hypernuclei, so the binding energies were estimated from a systematics of the ground state energies of light Λ-hypernuclei. The energies labeled $^8\mathrm{He} + \Lambda$ and $^3\mathrm{H} + 2n + \Lambda$ correspond to the thresholds of the quasi-free process. So, the energy separation

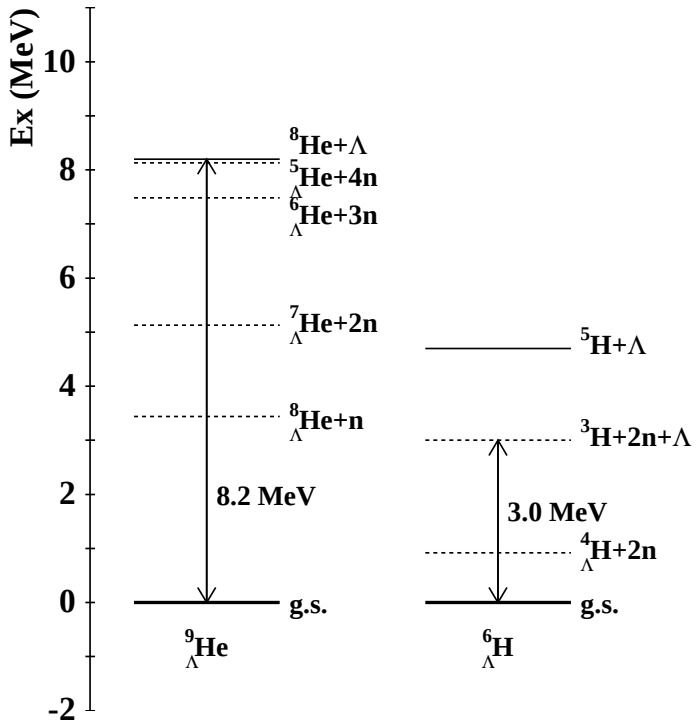

Figure 1: Threshold energies measured from the ground states for the ${}^{9}_{\Lambda}$He (left) and ${}^{6}_{\Lambda}$H (right) hypernuclei. The energy labeled ${}^{8}\mathrm{He}+\Lambda$ and ${}^{3}\mathrm{H}+2n+\Lambda$ correspond to the quasi-free thresholds.

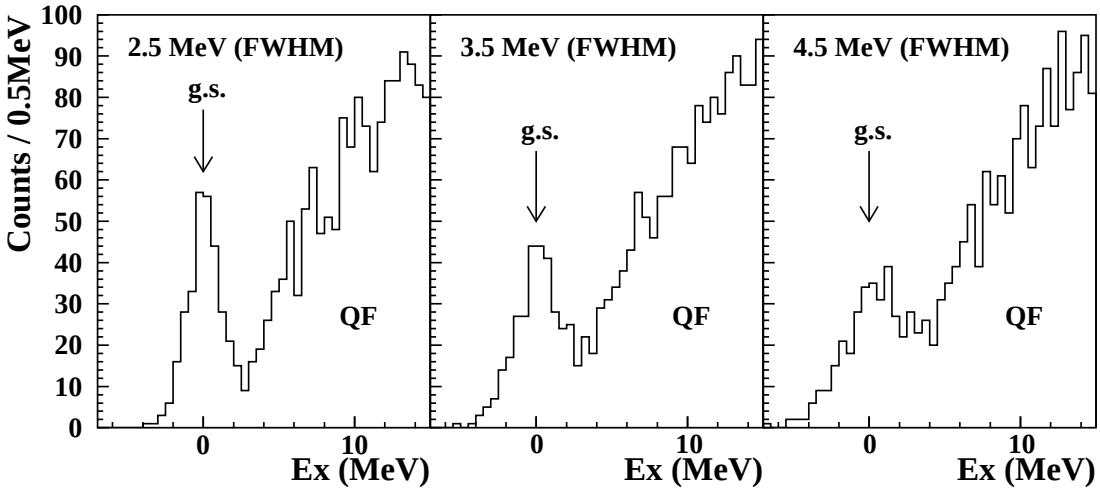

Figure 2: Simulated excitation energy spectra by assuming energy resolutions 2.5 MeV (left), 3.5 MeV (middle) and 4.5 MeV (right) in FWHM. The number of events for the ground state population is fixed to 300. See text for more details.

between the ground state and the quasi-free threshold energy is estimated to be about 3.0 MeV for the ${}^{6}_{\Lambda}$H hypernucleus.

Figure 2 shows simulated excitation energy spectra for the ${}^{6}_{\Lambda}$H production by assuming energy resolutions of 2.5 MeV, 3.5 MeV and 4.5 MeV (FWHM) from left to right. The yields of the ground state peaks are fixed to 300 events, and the yields of the quasi-free process up to 20 MeV excitation are assumed to be 10 times larger than that of the ground states. A Gaussian shape is assumed for the ground state peaks. With the 2.5 MeV resolution, the ground state peak is well separated from the contribution of the quasi-free process. The result with the 3.5 MeV resolution shows that the ground state peak is distinguishable from the quasi-free contribution, but the overlapping of the two components is considerably large. The parameters we employed; e.g., the binding energy of the ground state, the yield ratio between the ground state peak and the quasi-free process, and the shape of the response function of the spectrometer system may have some ambiguities. So, to stand on the safety side, we require the resolution of excitation energy of about 2.5 MeV (FWHM) for the E10 experiment.

The experimental energy resolution is discussed in more detail in Sec.3.1.

1.3 Energy resolution for binding energy determination

The precision of the binding energy determination is also an important factor of the E10 experiment. There are theoretical predictions that an interesting phenomena so-called "ΛN-ΣN mixing" is important in the structures of the neutron-rich hypernuclei. Akaishi, *et al.*, pointed out that the coherent ΛN-ΣN mixing (ΛNN

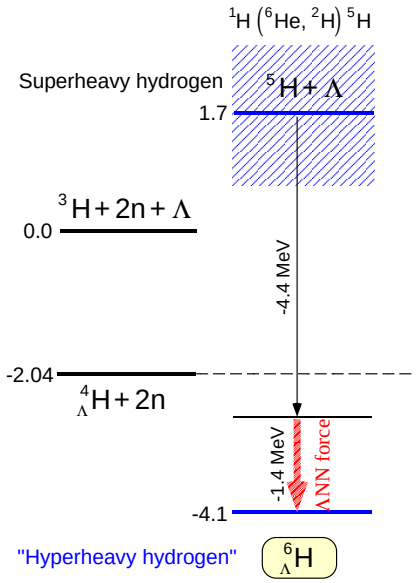

Figure 3: A theoretical prediction of the structure of the $^{6}_{\Lambda}$H hypernucleus by Akaishi, *et al.* [3]. A coherent ΛN-ΣN mixing effect (ΛNN 3-body force) increases the ground state binding energy of the neutron-rich hypernucleus by 1.4 MeV.

3-body force) may increase the binding energy of the $^{6}_{\Lambda}$H hypernucleus by 1.4 MeV (see Fig.3) [3]. A similar effect is expected also in the structure of the $^{9}_{\Lambda}$He hypernucleus. To see this interesting phenomena, we need a binding energy resolution better than 1 MeV for the hypernuclei.

We can estimate the binding energy resolution (ΔBE) by using the yield and the spectrometer resolution we required in Secs.1.1 and 1.2.

$$\Delta BE = \frac{2.5MeV}{\sqrt{300}} \sim 0.15MeV(FWHM)$$

The resolution is good enough for the detailed studies on the "ΛN-ΣN mixing" effects in the neutron-rich hypernuclei. In other words, the achievement of the yield of about 300 and the spectrometer resolution of about 2.5 MeV (FWHM) are indispensable for the E10 experiment.

2 K1.8 Beam Line and Beam Line Spectrometer

2.1 Basic performance of the K1.8 beam line

The performances of the K1.8 beam line and the beam line spectrometer are described in detail in the report for J-PARC FIFC by the J-PARC Hadron Beam Line Group [4]. The floor plan is shown in Fig.4. The primary target area of the K1.8

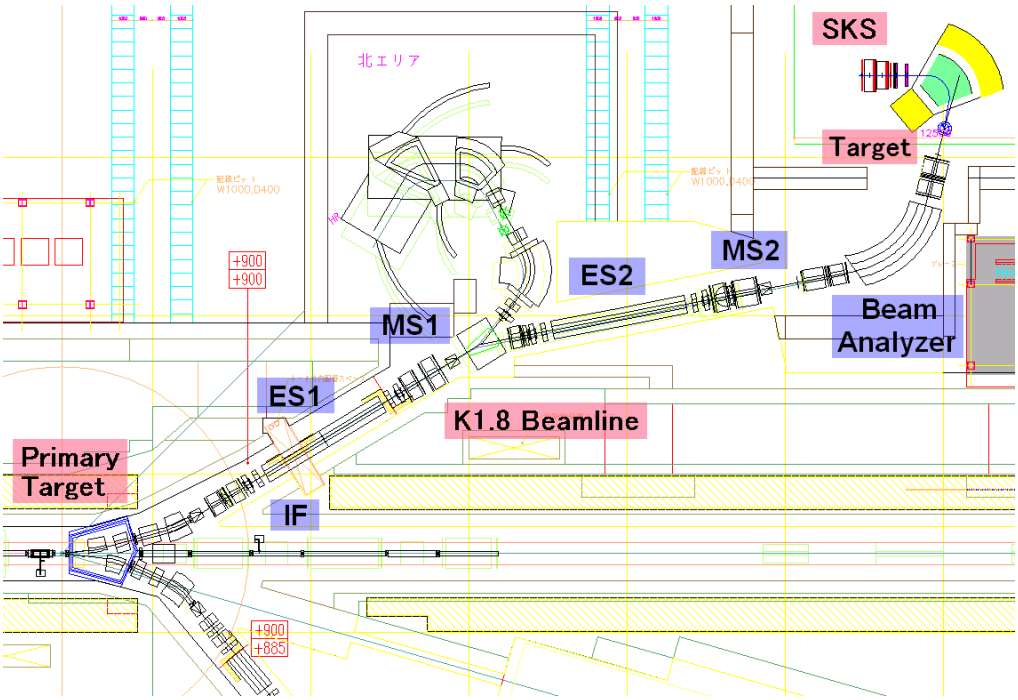

Figure 4: Layout of the K1.8 beam line and the beam line spectrometer.

beam line is designed carefully to handle the high power primary proton beam, 30GeV×9μA=270kW even in Phase I. At the same time, an excellent kaon/pion separation is achieved by the double-stage electro-static separators (ES1 and ES2) with an intermediate focus (IF) beam optics which reduce so-called "cloud pions" efficiently in the case of the kaon beam transport [5, 6].

Momenta of beam particles are measured by the beam line analyzer with a QQDQQ magnet configuration. Since a point-to-point optics is realized between the entrance and the exit of the QQDQQ system, the multiple scattering of a particle does not affect the momentum resolution in the first order, and an excellent momentum resolution, $\Delta p/p = 1.4 \times 10^{-4}$ in rms, is obtained. The K1.8 beam line and its beam line spectrometer provide us intense kaon beams, $1.4{\times}10^6$ K^-/spill at the experimental target with the 270 kW primary proton beams, in keeping the kaon/pion ratio close to 7.

A beam tracking system in the beam line spectrometer is necessary to obtain the beam momentum and the time-of-flight information. The standard tracking system

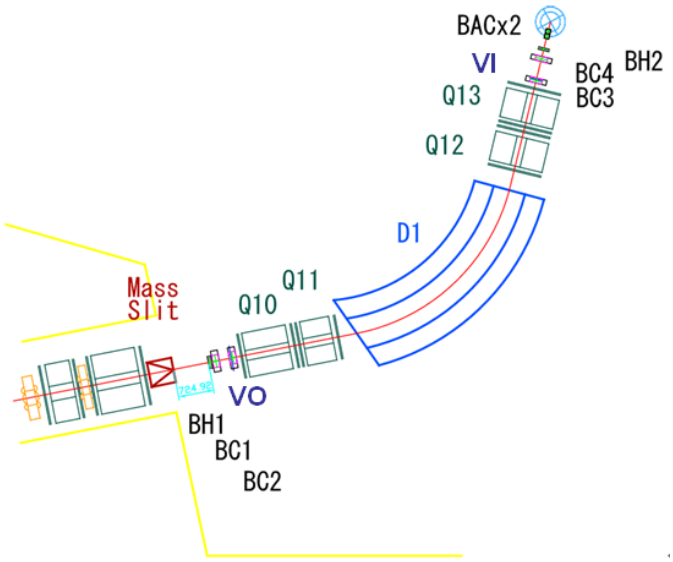

Figure 5: Layout of the beam line spectrometer of the K1.8 beam line. The beam line spectrometer has 4 tracking chambers for the momentum determination, BC1–4, and 2 beam hodoscopes for the time-of-flight measurement, BH1 and 2.

of the beam line spectrometer was discussed by the J-PARC E05 collaboration in the FIFC meeting [7]. Figure 5 shows the layout of the beam tracking system. The beam tracking system consists of 1 mm wire-spacing MWPC (BC1 and 2), 3 mm wire-spacing drift chambers (BC3 and 4) and segmented beam line hodoscopes (BH1 and 2). The detector combination was optimized for the E05 experiment that uses high intensity kaon beams.

The performances of the K1.8 beam line and the beam line spectrometer are suitable also for experiments for hypernuclear studies with pion beams. We expect to obtain clean pion beams due to the good performance of the double-stage electro-static beam separators. The excellent momentum resolution of the beam line spectrometer is essential for the hypernuclear studies which need at least a few MeV excitation energy resolution.

2.2 Consideration for E10

For the E10 experiment, we need very high intensity pion beams to override the very small production cross section of the double charge-exchange (π^-, K^+) reaction. In the yield estimation in Sec.1.1, we assumed the beam intensity of 10^7 pions/spill on the target. The use of such high intensity pion beams has not been established yet at BNL-AGS nor KEK-PS for hypernuclear experiments, so we need careful estimation on the feasibility of experiments with such high intensity beams in the K1.8 beam line at J-PARC. Here we discuss the performance of the beam line tracking chambers (BC1–4) and the performance of the beam line hodoscopes (BH1 and 2) at the high

Table 3: Beam spill length necessary to fulfil the chamber hit rates less than 200k hits/s/wire and the beam intensity 10^7 pions/spill at the same time. The standard configuration of the tracking chambers in the K1.8 beam line is assumed. The last line shows an estimation with the replacement of BC4 by the 1 mm MWPC same as BC1.

		maximum hit rate		
chambers	wire spacing	hit/mm/$10^7\pi$	hit/wire/$10^7\pi$	spill length
BC1	1 mm	400k	400k	2.00 s
BC2	1 mm	140k	140k	0.70 s
BC3	3 mm	150k	450k	2.25 s
BC4	3 mm	330k	990k	4.95 s
(BC4)	(1 mm)	330k	330k	1.65 s

counting rate.

2.2.1 Beam line tracking chambers

For the beam line tracking gas chambers, the maximum counting rate per sense wire was estimated to be 200k hits/s in the E05 report for FIFC [7]. The number came from the experience in the experiments at the KEK-PS K6 beam line. Although FIFC recommended to set the maximum counting rate of chambers to 100k hits/s/wire for more stable operation, we use the rate 200k hits/s/wire as a reference number in the following discussions. To estimate the counting rates of wires of the beam line tracking chambers, we calculated the hit rate of pion beams per unit length at each tracking chamber (BC1–4). Since a x-u-v wire configuration is used for the tracking chambers, the estimation is made for the x direction by using the MC ray-tracing program Decay TURTLE [8].

Figure 6 shows the beam hit number per 1 mm per 10M pion beams on the experimental target as a function of the x position of each tracking chamber. The black and red plots show the profiles of the pion beams and the decay muons, respectively. As one can see, the hit rate is high for the BC1 and BC4 tracking chambers because these chambers are close to the beam focal points. If we assume the standard 0.7 s beam spill length of the slow beam extraction, the hit rates of BC1, BC3 and BC4 are too high. On the other hand, if we set the maximum counting rate 200k hits/s/wire, we can estimate the minimum beam spill length to fulfill the condition as shown in Table 3. In the estimation, we employ the standard chamber configuration of the K1.8 beam line described in Sec.2.1, 1 mm wire-spacing for BC1 and 2 and 3 mm wire-spacing for BC3 and 4. We also assume the beam intensity of 10M pions/spill as written in the proposal. The slow beam extraction system is currently designed to be able to extend the beam spill up to 3 s in the case of the PS operation at the 30 GeV beam energy. So, spill duration longer than 2 s is adequate for the operation of the K1.8 standard BC1, BC2 and BC3 tracking

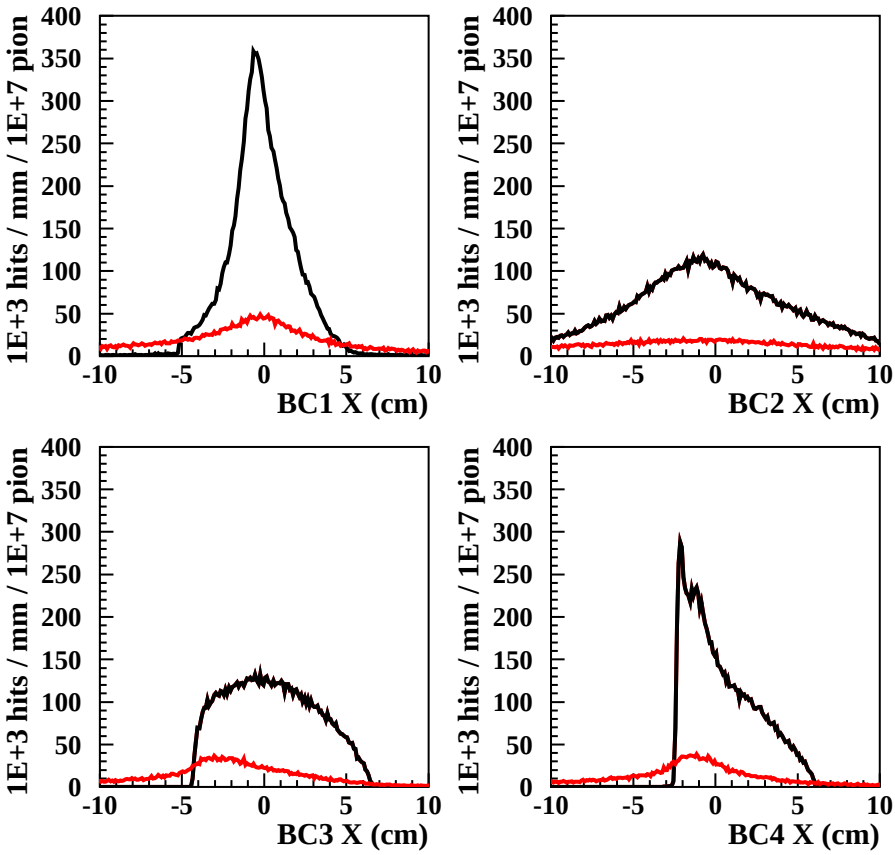

Figure 6: Counting rate of x wires at each beam line chamber (BC1, 2, 3 and 4) per 1 mm per 10M pions on the target. The black and red plots show the profiles of the pion beams and the decay muons, respectively.

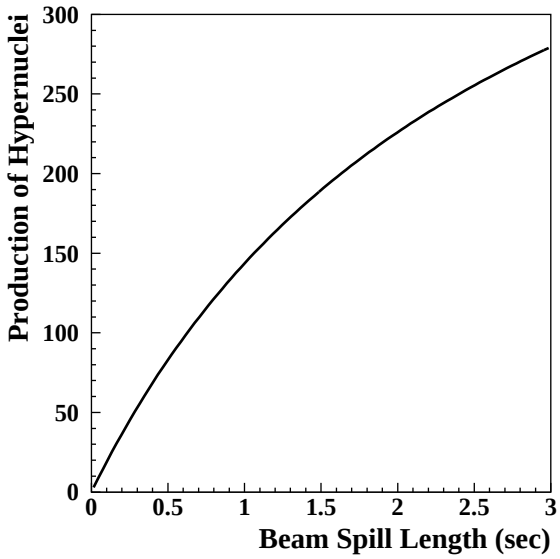

Figure 7: Result of re-estimation of the yield of the ${}^{9}_{\Lambda}$He hypernucleus as a function of the beam spill length by using the realistic beam intensity.

chambers, and the replacement of BC4 is necessary for the E10 experiment. Figure 7 shows a result of a re-estimation of the yield for the ${}^{9}_{\Lambda}$He hypernucleus production as a function of beam spill length by using the realistic beam intensity. We assumed the beam intensity of 5M pions/s (10M pions in 2 s) on the target in the estimation.

A candidate of the BC4 replacement is a 1 mm wire-spacing MWPC same as BC1 as listed in the last line of Table 3. We believe there are several options for the BC4 replacement.

1. A low cost option is the exchange of BC2 and BC4. We need negotiation with the E05 collaboration.

2. Another option is a fabrication of a new 1 mm MWPC similar with BC1 and BC2. We need some amount of cost for the chamber fabrication and readout system. We need an additional budget or a cost sharing with other K1.8 user groups.

3. Development of other types of tracking chambers for the operation in the high rate environment. A chamber based on the GEM technique is a candidate. Osaka Electro-Communication University group has experience on GEM based chambers, but some R&D works are necessary for the E10 experiment.

We are planning to select one of the options depending on the performances we require and the costs needed for detector updates. We need further discussions with other K1.8 experimental groups.

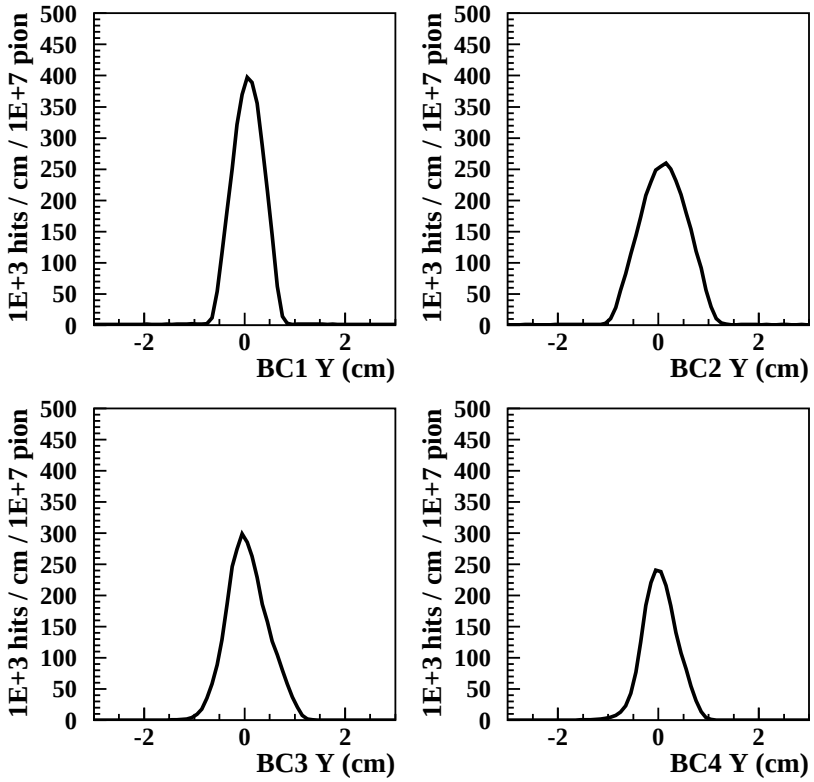

Figure 8: Estimation of beam hit rates of BCs per 1 cm per 10^7 pions on the target as functions of y positions at BCs.

2.2.2 Space charge effect

The effect of the space charge in the K1.8 beam line chambers was discussed by the E05 collaboration. They estimated that the effect was about 60 % gain drop at 100k hits/s/5mm (= 200k hits/s/cm) for a wire based on the rate dependence of chamber gains reported in Ref.[9].

Figure 8 shows an estimation of the maximum beam hit rates of BCs per 1 cm per 10^7 pions on the target as functions of y positions at BCs. In the estimation, the contribution of decay muons is ignored because the total amount of the decay muons is 10 % level and x and y distributions of the muons are broad. Relatively tight mass slit (MS1 and MS2) settings are used which are suitable for the kaon beam transport with good kaon/pion ratio. If we assume 2 s beam spill for the slow extraction of pion beams as we discussed above, the maximum rate per unit length is about 200k hits/s/cm (BC1 case). So, the situation is similar with that of the E05 experiment.

Further, we believe we can reduce the beam hit rates by combinations of following changes:

Table 4: Designs of the standard beam hodoscope detectors written in Ref.[7].

hodoscope	segmentation	area of detector
BH1	11	150mm(W)×60mm(H)
BH2	5	150mm(W)×60mm(H)

- The widths of the y distributions are determined by the widths of the slits (IF, MS1 and MS2), and we can make the tuning of slits to optimize the beam widths in the y direction and the pion/kaon separation. In the case of the pion beams especially for the negative pions, the separation of $\pi^-/K^-/\bar{p}$ is relatively easy. The lower beam momentum, 1.2 GeV/c, also helps the separation.

- The change of the BC1 and BC4 positions affect to the hit rates per wire. We can optimize the positions of these tracking chambers by looking at the beam hit rates and the momentum resolution of the beam line spectrometer. Although the change of the chamber positions may deteriorate the momentum resolution of the beam line spectrometer, the overall energy resolution is mainly determined by the SKS momentum resolution and the thickness of the target. So, we believe we have a room to change the tracking chamber positions.

- Beam defocus by the Q-magnets. This affects especially to the beam profiles at DC1 and DC2 to be discussed in Sec.3.3. The change may affect to the momentum resolution of the beam line spectrometer.

2.2.3 Beam line hodoscopes

In the E10 experiment, the counting rates of beam line hodoscopes, BH1 and BH2, are also high. The standard BHs for the K1.8 beam line will be prepared by the E05 collaboration, and these are segmented plastic scintillation counters. The designs of the standard beam line hodoscopes written in the E05 report [7] are listed in Table 4. The adjustment of the BH module widths was considered by taking into account the beam intensity and the shape of the beam profiles at BH1 and BH2.

The rate capability of the plastic scintillation detectors was studied with beams at KEK-PS [10]. A small size plastic scintillator, 40mm×60mm, was read out by two dynode-boosted PMTs in the beam test. The typical timing resolution for the small size plastic scintillators was 30–40 ps (rms) for MIP particles, and the deterioration of the timing resolution was not significant up to a few 10^6 hits/s.

If we assume the 2 s of beam spill length as we discussed in Sec.2.2.1, the maximum beam rate is about 200k particles/s/mm. We refer the beam profiles at BC1 and BC4 because the positions of BHs are close to the beam line chambers. This result means the maximum width of the BH modules is about 10 mm by the

consideration of the sustainable hit rate. By taking into account the shape of the beams, we can use BH1 without any modifications for the E10 experiment, and we need to update BH2 to increase the number of the segmentation.

The lifetime of the scintillators of the beam line hodoscopes is estimated to be about 5–10 years from the experience at the KEK-PS K6 beam line. So, any frequent maintenance is not necessary for BHs.

2.2.4 Effects of beam micro structure

In the estimations above, we assumed stable beam rates during the spill of the slow beam extraction. If the beam has some micro structure during the extraction, the beam rate may exceed the maximum rate we are assuming, and detector inefficiencies and deteriorations of performances arise. So, the control of the spill is an important issue for this type of experiments.

A spill control system for the slow extraction by the feedback and the feedforward methods are under development by the accelerator group. Current plan of the development do not assume operation of the control system at Day-1 because they assume a low primary proton beam intensity at Day-1. But experiments with intense pion beams need the stable beam spill, so we have to continue discussions and collaborations with the accelerator group.

3 SKS Spectrometer

We will use the Superconducting Kaon Spectrometer (SKS) [11] for the detection of K^+ in the E10 experiment. Figure 9 shows the layout of SKS that consists of a superconducting magnet (B_{max}=3T) and a detector system for the K^+ tracking and identification. The tracking system consists of 2 small drift chambers at the

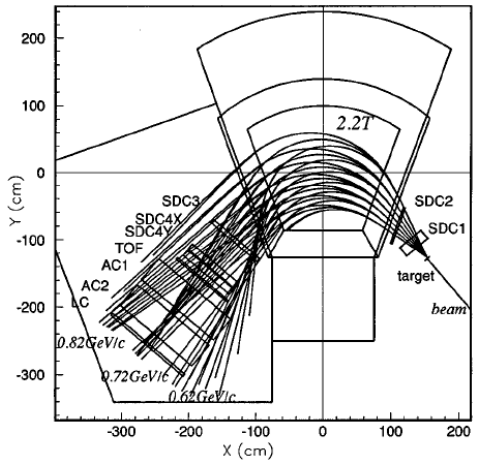

Figure 9: Superconducting Kaon Spectrometer (SKS) consists of a superconducting magnet and K^+ tracking and identification detectors.

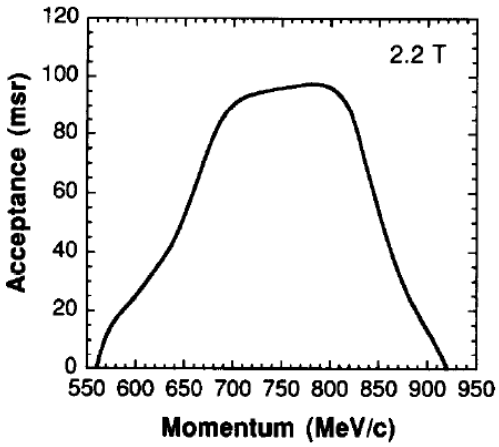

Figure 10: SKS angular acceptance as a function of kaon momentum for an excitation at a 2.2 T magnetic field.

magnet entrance, SDC1 and 2, and 2 drift chambers at the exit, SDC3 and SDC4. SKS has an excellent momentum resolution, $\Delta p/p$=10^{-3} (FWHM) at 0.72 GeV/c, and a large angular acceptance, about 100 msr (see Fig.10). The large angular acceptance is necessary for the E10 experiment because the cross section of the double charge-exchange (π^-, K^+) reaction is tiny in comparison with the ordinary non charge-exchange (π^+, K^+) reaction.

3.1 Overall energy resolution

The good momentum resolution is suitable for the hypernuclear studies which require a few MeV (FWHM) level of the excitation energy resolution by the missing mass spectroscopy. Figure 11 shows a typical binding energy spectrum obtained with SKS at the KEK-PS K6 beam line by the ordinary (π^+, K^+) reaction [12].

In a practical experiment with a thick target, the overall excitation energy resolution depends also on the target thickness through the energy loss and the multiple scattering processes. Figure 12 is a summary of the excitation energy resolution achieved in experiments at the KEK-PS K6 beam line as a function of the target thickness. The circles show the data points for C (blue), Y (light blue), La (purple), Pb (red), B and Li (open circles) targets. The energy resolutions are mainly

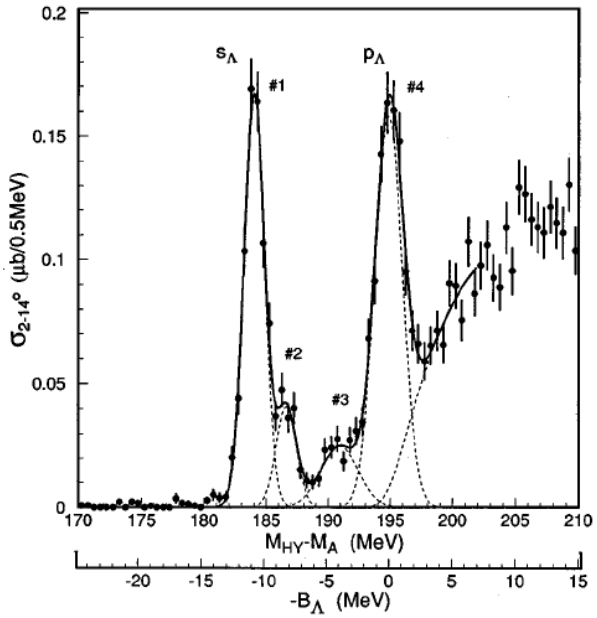

Figure 11: A typical binding energy spectrum obtained with SKS at the KEK-PS K6 beam line by the ordinary (π^+, K^+) reaction [12]. The peaks correspond to states in the ${}^{12}_{\Lambda}$C hypernucleus.

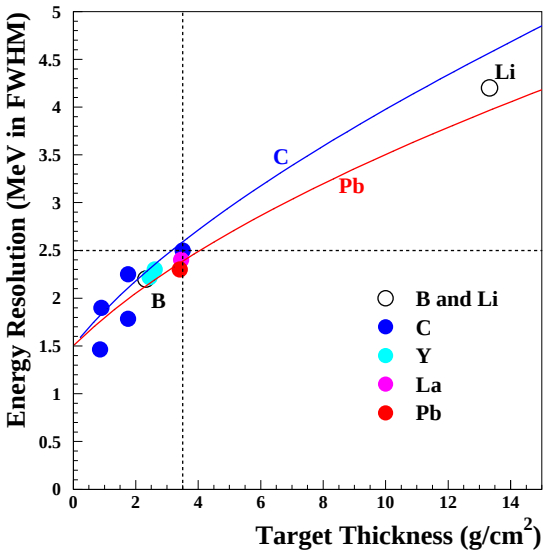

Figure 12: Summary of the overall excitation energy resolution achieved in experiments at the KEK-PS K6 beam line as a function of the target thickness. See text for more details.

determined by the energy loss straggling of pion and kaon in the target, and the target thickness dependence of the resolution is well reproduced by a simple model calculation considering the intrinsic SKS resolution and effects of the energy loss and the multiple scattering in the target (solid curves in Fig.12). As discussed in Sec.1.2, we need excitation energy resolution better than 2.5 MeV (FWHM) for the E10 experiment. So, we will use ^{9}Be and ^{6}Li targets with about 3.5 g/cm^2 thicknesses.

3.2 Calibration of binding energy

By using SKS, we can distinguish the ground state peak from the quasi-free process background very clearly. Another issue is the calibration of the absolute value of the binding energy for the ground state of the neutron-rich hypernuclei. For the ordinary non charge-exchange (π^+, K^+) reaction, we can have reference peaks in the excitation energy spectrum because we have information on the binding energies for several hypernuclei from the emulsion experiments. The situation is quite different in the neutron-rich hypernuclei. Most of the neutron-rich hypernuclei are to be produced for the first time, so we have almost no information on the binding energies of hypernuclei. The binding energy should be estimated from momenta measured by the beam line spectrometer and SKS. We are planning to employ following procedures to calibrate the binding energy:

- For the calibration of SKS, we can use the ordinary (π^+, K^+) reaction. Since the binding energy of $^{12}_{\Lambda}$C hypernucleus is well known, we wish to use the ground state peak of the hypernucleus as a reference.

- To measure the (π^-, K^+) reaction, we have to change the polarity of the K1.8 beam line magnets. The polarity change does not affect much on the momentum determination in the beam line spectrometer if the fields of the K1.8 beam line elements are set properly. The phase space distributions of the π^- and π^+ beams are considered to be similar. So, remaining ambiguities of the binding energy determination are the 2nd order.

- The effect of the beam line polarity change can be checked by the comparison of the $p(\pi^+, K^+)\Sigma^+$ and the $p(\pi^-, K^+)\Sigma^-$ reactions. We are planning to use a CH_2 target for the calibration runs.

- The magnetic field strengths of the dipole magnet of the beam line spectrometer and SKS are monitored by hole probes and/or NMR probes regularly during the beamtime.

We have to make several studies on the feasibility of the procedures during the commissioning of the K1.8 beam line.

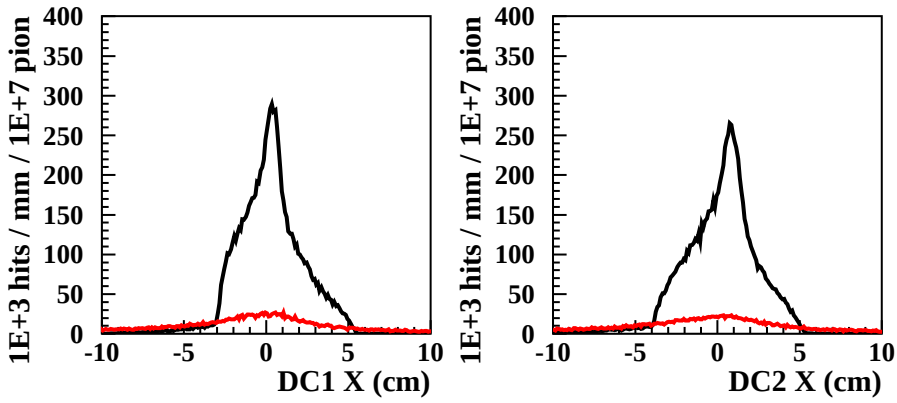

Figure 13: Counting rate of x wires of the SKS drift chambers (DC1 and DC2) per 1 mm per 10M pions on the target. The black and red plots show the profiles of the pion beams and the decay muons, respectively.

3.3 Operation at high beam intensity

Since the drift chambers at the entrance of SKS, SDC1 and 2, are close to the target, we have to consider the rate capability for these tracking detectors. Figure 13 shows the beam hit rates for SDC1 and SDC2 (these are renamed to DC1 and DC2 at J-PARC). The black and red plots show the profiles of the pion beam and the decay muons, respectively, at DC1 and DC2. The beam hit rates are close to that of the BC1 and BC4, so we need replacement of the standard DCs (3 mm wire-spacing drift chambers) by tracking detectors with higher rate capabilities. The beam spill length necessary to operate the standard DCs and replaced detectors are listed in Table 5. The assumptions of calculation for Table 5 are same as those for Table 3.

Table 5: Beam spill length necessary to fulfil the chamber hit rates less than 200k hits/s/wire and 10^7 pions/spill at the same time. The standard configuration of the tracking chambers of SKS is assumed for the 1st and 2nd lines. The 3rd and 4th lines show an estimation with the replacement of DCs by 1 mm wire-spacing chambers.

		maximum hit rate		
chambers	wire spacing	hit/mm/$10^7\pi$	hit/wire/$10^7\pi$	spill length
DC1	3 mm	310k	930k	4.65 s
DC2	3 mm	290k	870k	4.35 s
(DC1)	(1 mm)	310k	310k	1.55 s
(DC2)	(1 mm)	290k	290k	1.45 s

4 Safety Issues

4.1 Radiation protection

In the E10 experiment, the intense pion beams come to the experimental target, and the same order of decay muons are also come to the experimental area. So, the whole experimental area will be surrounded by the radiation shield as already discussed in the report of the E05 experiment [7]. The hadron experimental hall itself was designed with consideration on the construction of the radiation shield.

4.2 Toxic and flammable materials

We will use a metallic ^{9}Be target. Although the beryllium is a toxic material, the risk of hazards during the experiment is expected to be low for the metallic beryllium plate if the target plate is kept in a air tight package. Special cares have to be payed at the installation and uninstallation of the beryllium target.

A metallic ^{6}Li target is also used in the E10 experiment. The metallic lithium is chemically active and flammable in the air, so a careful treatment is necessary. We are planning to seal the lithium to isolate it from the air, and the sealed lithium will be kept in an Ar gas environment during the experiment.

The wire chamber gas are flammable. Exhaust pipes from the K1.8 beam line area to the outside of the hadron hall will be reserved for the chamber gas. Gas leak detectors will be set around the gas handling system for the chambers.

4.3 Cryogenic system for SKS

As reported by the E05 collaboration, SKS will be transferred from KEK to J-PARC in the fiscal year 2008 and the cryogenic system will be updated [7]. The design of the new cryogenic system with GM-JT 4K cryocoolers is more simple in comparison with that of old system at KEK-PS, and we expect a stable operation of the SKS cryogenic system at J-PARC.

Since the cryogenic system is operated for 24 hours a day, the system will be designed and operated as follows:

- A leak valve is attached to the cryogenic system to evacuate He gas when liquid He is evaporated due to some accidents, like a refrigerator trouble or a power failure. For the evacuation, an exhaust duct to the outside of the hadron hall is prepared for the evaporated He gas.
- Regular monitoring of the status of the cryogenic system locally and remotely.
- Regular system check by shift members.
- Monitoring of the oxygen level to avoid suffocation.

4.4 Operation of SKS magnet

During the SKS magnet turned on, persons are assigned as shift members of the magnet operation as it was at the KEK-PS K6 beam line. Trainings are required for the shift members to be able to take proper action to the magnet quenching, etc.

5 Cost and Budget

5.1 Cost estimation

The equipments necessary to pursue the E10 experiment are the K1.8 beam line and SKS only. That means most of the equipments necessary for the E10 experiment will be prepared as the standard setup of the K1.8 beam line and SKS. So, we list up costs for only additional equipments specific for the E10 experiments in Table 6. In the estimation, we assumed the option 1, the low cost option, discussed in Sec.2.2.1.

Table 6: Cost estimation for the E10 experiment.

item	unit cost (JPY)	units	total cost (JPY)
DC1, DC2 update	5,000,000	2	10,000,000
electronics for chamber	8,000,000	2	16,000,000
BH2 update	2,000,000	1	2,000,000
total			28,000,000

5.2 Status of budget

The E10 experiment is supported by the Grant-In-Aid Priority Area "Multi-quark systems with strangeness" from Japanese Ministry of Education, Culture, Sports, Science and Technology (MEXT). The budget profile is listed in Table 7. We wish to note that the J-PARC E22 experiment also relies on the same budget from MEXT. Although we have to consider costs of both experiments, the costs listed in Table 6 is within the capacity of the budget.

If we assume updates of other detectors like BC4, we need collaboration with other experiments; e.g., the E05 and the E19 collaborations, to share the costs for the preparation of the experiments.

Table 7: Profile of budget from Grant-In-Aid Priority Area.

fiscal year	budget (JPY)
2005	3,600,000
2006	6,500,000
2007	47,300,000
2008	29,000,000
2009	2,700,000
total	89,100,000

6 Time Schedule

Figure 14 shows the schedule of the preparation related to the E10 experiment. The table also includes the schedules of the K1.8 beam line and SKS installations by the Hadron Beam Line Group and the E05 collaboration.

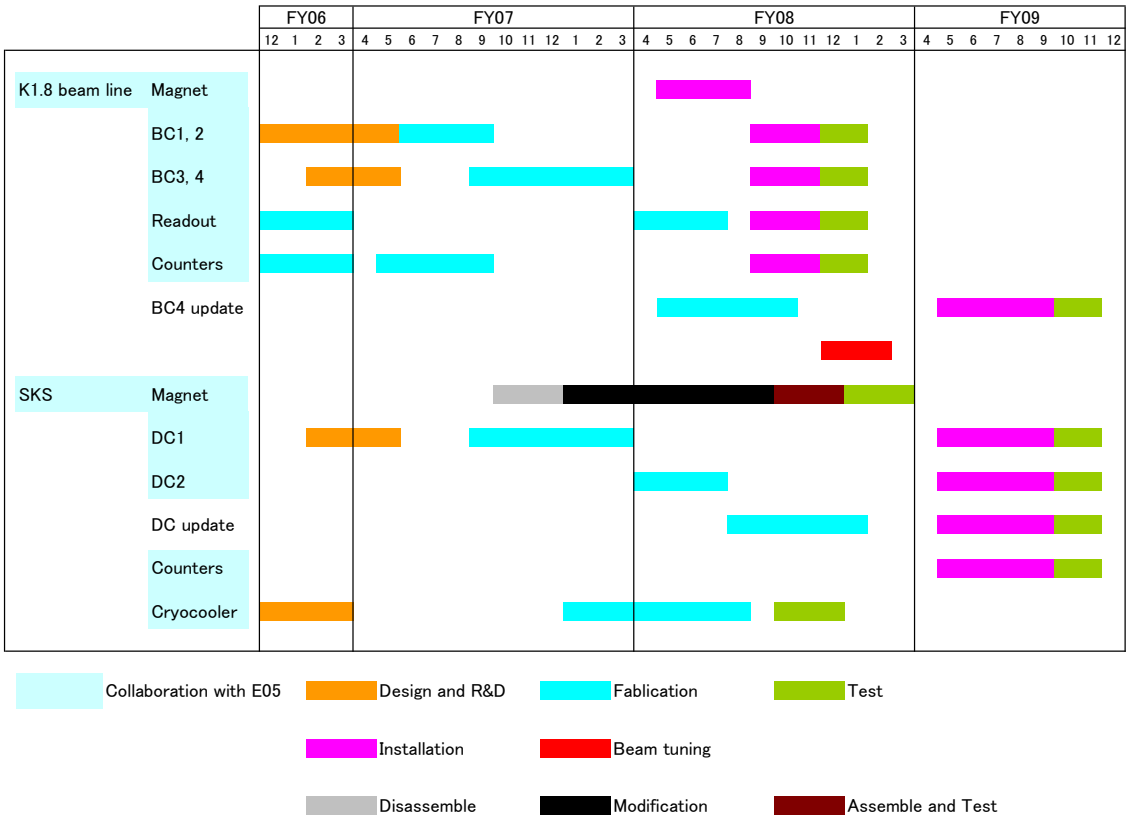

Figure 14: Schedule of preparation related to the E10 experiment.

7 Collaboration

Table 8 shows a list of collaboration. The major preparation of the beam line spectrometer and SKS will be done in collaboration with the Hadron Beam Line Group, the E05 group and other K1.8 user groups.

Table 8: List of collaboration.

Institution	Member
Osaka University	Atsushi Sakaguchi*
	Shuhei Ajimura
	Tadafumi Kishimoto
Osaka Electro-Communication University	Tomokazu Fukuda*
	Yutaka Mizoi
KEK	Toshiyuki Takahashi
	Hiroyuki Noumi
JAEA	Pranab Kumar Saha
Seoul National University, Korea	Hyoung Chan Bhang
Università di Torino, Italy	Luigi Busso
INFN, Italy	Diego Faso
INAF-IFSI, Italy	Ombretta Morra

An E10 specific issue is the update of BC4, DC1 and DC2 tracking chambers. Osaka University will contribute largely to the update based on the 1 mm MWPC similar with the BC1 and BC2 chambers to be developed by the E05 collaboration. Osaka Electro-Communication University will contribute to R&D works on GEM based high rate gas chambers.

KEK will contribute to the optimization of the beam optics of the K1.8 beam line and the beam line spectrometer for the E10 experiment. All institutes will contribute to carry out the beamtime and analyses.

References

[1] S. Ajimura, *et al.*, J-PARC E10 Collaboration, J-PARC 50 GeV PS proposal P10 "Production of Neutron-Rich Λ-Hypernuclei with the Double Charge-Exchange Reaction".

[2] P.K. Saha, *et al.*, KEK-PS-E521 Collaboration, Phys. Rev. Lett. **94** (2005) 052502.

[3] Y. Akaishi, *et al.*, Frascati Physics Series, Vol. XVI, pp. 59-74 (1999); private communication, 2001-2002.

[4] J-PARC Hadron Beam Line Group, "Report on the K1.8 bram line", report prepared for J-PARC FIFC meeting in 2006.

[5] M. Takasaki, *et al.*, Nucl. Inst. Meth. **A242** (1986) 201.

[6] P.H. Pile, *et al.*, Nucl. Inst. Meth. **A321** (1992) 48.

[7] E05 Collaboration, "Report on status of J-PARC E05 experiment", report prepared for the FIFC meeting in 2006.

[8] K.L. Brown, Ch. Iselin, D.C. Carey, Decay Turtle, CERN 74-2 (1974); PSI Graphic Turtle Framework by U. Rohrer based on a CERN-SLAC-FERMILAB version.

[9] M. Aleksa, *et al.*, Nucl. Instr. Meth. **A446** (2000) 435.

[10] Y.D. Kim, H. Bhang, O. Hashimoto, K. Maeda, K. Omata, H. Outa, H. Park and M. Youn, Nucl. Instr. Meth. **A372** (1996) 431.

[11] T. Fukuda, *et al.*, Nucl. Instrm. Meth. **A361** (1995) 485.

[12] T. Hasegawa, *et al.*, Phys. Rev. **C53** (1996) 1210.